Carcinogenesis vol.34 no.4 pp.841–849, 2013
doi:10.1093/carcin/bgs390
Advance Access publication December 13, 2012

Chemoprevention of lung tumorigenesis by intranasally administered diindolylmethane in A/J mice

Xuemin Qian[1], Jung Min Song[1], Tamene Melkamu[2], Pramod Upadhyaya[1] and Fekadu Kassie[1,3,*]

[1]Department of Veterinary Clinical Sciences Masonic Cancer Center, [2]Department of Animal Science, College of Agriculture and [3]Department of Veterinary Clinical Sciences College of Veterinary Medicine, University of Minnesota, Minneapolis, MN 55455, USA

*To whom correspondence should be addressed. Masonic Cancer Center, University of Minnesota, Mayo Mail Code 806, 420 Delaware Street SE, Minneapolis, MN 55455, USA. Tel: +612-625-9637; Fax: +612-626-5135; Email: kassi012@umn.edu

The main reasons for the failure of most chemopreventive agents during clinical trials are poor *in vivo* bioavailability and dose-limiting side effects. One potential approach to surmount these problems in lung cancer chemoprevention trials could be direct delivery of agents into the pulmonary tissue. In this study, we assessed the efficacy of intranasally delivered bio-response diindolylmethane (BRD) against 4-(methylnitrosamino)-1-(3-pyridyl)-1-butanone (NNK)-induced lung tumorigenesis in mice. Mice treated with NNK (two doses of 50 mg/kg at an interval of a week, intraperitoneal) developed 16.3 ± 2.9 lung tumors per mouse. Post-carcinogen administration of BRD, via intranasal instillation, for 24 weeks, twice a week, at a dose of 2 mg per mouse (0.6 mg pure diindolylmethane per mouse) reduced the lung tumor multiplicity to 4.6 ± 2.2 tumors per mouse (72% reduction). Likewise, large tumors (>1 mm) were almost completely abolished and multiplicities of tumors with a size of 0.5–1 mm were reduced by 74%. Tumor volume was also reduced by 82%. Further studies using an *in vitro* model of lung tumorigenesis showed that BRD exhibited pronounced antiproliferative and apoptotic effects in premalignant and malignant bronchial cells but only minimal effects in parental immortalized cells through, at least in part, suppression of the phosphatidylinositol 3-kinase (PI3K)/Akt signaling pathway. These results showed the potent lung tumor inhibitory activities of low doses of BRD given via intranasal instillation and, therefore, intranasal delivery of BRD holds a great promise for lung cancer chemoprevention in subjects at high risk to develop lung cancer.

Introduction

Lung cancer is the most fatal malignancy in the USA in both men and women and an estimated 160 340 deaths, accounting for about 28% of all cancer cases, are expected to occur in 2012 (1). Despite significant advances in surgical, radiotherapeutic, chemotherapeutic and targeted treatment of lung cancer, the long-term survival of most patients remains low (2). The use of chemopreventive agents by apparently healthy former smokers or patients with resected lung tumors could be a viable strategy to inhibit the development to lung cancer. However, there is presently no clinically proven chemopreventive agent against lung cancer. This is, partly, due to low pulmonary bioavailability of most chemopreventive agents.

Diindolylmethane (DIM), the predominant acid-catalyzed condensation product of indole-3-carbinol, is a promising anticancer agent. Several studies in cell line and xenograft models have demonstrated that DIM suppresses growth of cancer cells and potentiates the effects of chemotherapeutic agents (3–10). Also, in murine models of early phase tumorigenesis, DIM has been shown to inhibit tumor formation in the prostate (11), cervix (12) and lung (13). Despite the promising anticancer effects of DIM, most of the preclinical studies in murine models have been carried out at dose levels that are at least one order of magnitude higher than the amount of DIM tolerated by humans. Another issue is the poor bioavailability of DIM. Administration of DIM to human volunteers at the maximum tolerated dose level (14) led to a plasma concentration that was two orders of magnitude less than the concentrations of the agent required to induce apoptotic and antiproliferative effects in cell line models (3).

In lung chemoprevention studies, one promising strategy to overcome the poor bioavailability and potential systemic toxicities of DIM is administration of the agent via the intranasal route, a non-invasive drug administration method, which enables direct delivery of the agent to the lung, thereby imparting optimal DIM concentration at the target organ but decreased exposure of non-target normal tissues. In this study, we examined the efficacy of intranasally administered bio-response DIM (BRD), absorption-enhanced DIM formulation, against 4-(methylnitrosamino)-1-(3-pyridyl)-1-butanone (NNK)-induced lung tumorigenesis in mice. Moreover, we assessed, using an *in vitro* model of lung tumorigenesis consisting of bronchial cells at different stages of transformation, the antiproliferative and apoptotic activities of BRD and the mechanisms through which these effects are mediated. Our findings indicate that intranasal administration of BRD, at dose levels equivalent to those found to be well tolerated in humans, significantly inhibited NNK-induced lung tumorigenesis in mice. Also, BRD differentially suppressed the growth and survival of premalignant and malignant bronchial cells with minimal effects in parental immortalized cells through, at least partly, inhibition of the phosphatidylinositol 3-kinase (PI3K)/Akt signaling pathway.

Materials and methods

Chemicals, reagents, plasmids and animal diets

BRD, absorption-enhanced formulation of DIM solubilized with phosphatidylcholine and microencapsulated in starch particles, was kindly provided by Dr Michael Zeligs (BioResponse, LLC, Boulder, CO). BRD contains 30% pure DIM but exhibits higher bioavailability than does crystalline DIM (15,16). NNK was synthesized as described previously (17). Anti-pEGFR, anti-pIGF1R, anti-pAkt, anti-Akt, anti-pGSK3b, anti-pNF-kB p65, anti-pJNK, anti-pP38, anti-pERK, anti-Bcl2, anti-Mcl-1, anti-PARP, anti-β-actin, goat antirabbit IgG secondary antibody, LY294002 and SP600125 were from Cell Signaling Technology (Beverly, MA). Mouse diets (AIN-93G and AIN-93M) were purchased from Harlan Teklad (Madison, WI). myr-HA-Akt1 (myr-Akt, constitutively active Akt) and control vector were kindly provided by Dr Lokeshwar (University of Florida School of Medicine). The AIN-93G diet, high in protein and fat, was used to support rapid growth of the mice until the animals became mature adults (16 weeks old); thereafter, AIN-93G diet was replaced by AIN-93M diet, a low-protein and low-fat diet, which is recommended for adult maintenance (18). AIN-93 diets are standard diets for lung tumorigenesis studies in A/J mice.

Cells and cell culture

Immortalized human bronchial cell line (BEAS-2B) and its premalignant (1799 and 1198) and malignant (1170) derivatives were kindly provided by Dr Klein-Szanto (Fox Chaser Cancer Center, Philadelphia). Cell line 1799 was developed from BEAS-2B cells explanted along with beeswax pellets into rat tracheas that had been denuded of bronchial epithelium and further transplanted into the dorsal subcutaneous tissues of nude mice (19). Cell lines 1198 and 1170 were developed in a similar manner except that the beeswax pellets contained cigarette smoke condensate. All bronchial cells were maintained in keratinocyte serum-free medium with recommended supplements (Life Technologies, Gaithersburg, MD) in a humidified atmosphere containing 5% CO_2. The cells were of the same passage number when used for the study.

Abbreviations: BRD, bio-response diindolylmethane; DIM, diindolylmethane; DMSO, dimethyl sulfoxide; EGFR, epidermal growth factor receptor; JNK, c-jun N-terminal kinase; NNK, 4-(methylnitrosamino)-1-(3-pyridyl)-1-butanone; PARP, poly (ADP ribose) polymerase; PI, propidium iodide; PI3K, phosphatidylinositol 3-kinase.

Cell proliferation assay

Cell growth was determined using the methylthiazoletetrazolium (Biotium, Hayward, CA) assay as follows. Parental BEAS-2B cells and its three derivatives were plated on a 96-well plate for 24 h and then exposed to BRD (5, 10 or 15 μM) for 72 h followed by methylthiazoletetrazolium treatment (100 μl per well) for 3 h. Subsequently, culture media were aspirated, 100 μl of dimethyl sulfoxide (DMSO) was added to each well and absorbance was read at 570 nm with a plate reader. Each treatment with DMSO or BRD was carried out in triplicate and the assays were repeated three times on different days.

Annexin V/propidium iodide assays for apoptosis

For annexin V/propidium iodide (PI) assays, cells were stained with annexin V-fluorescein isothiocyanate and PI and then evaluated for apoptosis by flow cytometry according to the manufacturer's protocol (BD Pharmingen, San Diego, CA). Briefly, after 1198 cells were pretreated with the vehicle (DMSO, 0.1%), or low concentrations of LY294002 (10 or 20 μM), or SP600125 (5 or 10 μM) for 1 h, cells were further exposed to DMSO or BRD (10 or 20 μM) for 24 h. Subsequently, cells were washed twice with cold phosphate-buffered saline and stained with 5 μl annexin V-fluorescein isothiocyanate and 10 μl PI (5 μg/ml) in 1× binding buffer [10 mmol/l *N*-2-hydroxyethylpiperazine-*N*′-2-ethanesulfonic acid (pH 7.4), 140 mmol/l NaOH, 2.5 mmol/l $CaCl_2$] for 15 min at room temperature in the dark. The apoptotic cells were determined using a Becton Dickinson FACScan cytofluorometer. Both early apoptotic (annexin V-positive and PI-negative) and late apoptotic (annexin V-positive and PI-positive) cells were included in cell death determinations.

Western immunoblot analyses

For the preparation of cell lysates, bronchial cells (1×10^6) treated with the various agents were harvested and suspended for 1 h in a lysis buffer composed of the following constituents: 50 mmol/l Tris–HCl, 150 mmol/l NaCl, 1 mmol/l ethyleneglycol-bis(aminoethylether)-tetraacetic acid, 1 mmol/l ethylenediaminetetraacetic acid, 20 mmol/l 1% Triton X-100 (pH 7.4), protease inhibitors [aprotinin (1 μg/ml), leupeptin (1 μg/ml), pepstatin (1 μmol/l) and phenylmethylsulfonyl fluoride (0.1 mmol/l)] and phosphatase inhibitors [Na_3VO_4 (1 mmol/l) and NaF (1 mmol/l)]. The preparations were centrifuged (14 000*g* for 25 min at 4°C), the supernatants were collected, aliquoted and stored at −80°C. For the preparation of mouse lung tissue lysates, aliquots of normal lungs (vehicle control mice, 30 mg per mouse) or microdissected tumors (carcinogen-treated mice, 30 mg per mouse) from the left lung lobe of six mice were pooled, ground with a mortar and pestle on liquid nitrogen and the powder suspended in ice-cold lysis buffer for 1 h and processed similar to the cell lysates.

For western immunoblotting, 60 μg of protein from the cell or tissue lysates were loaded onto a 4–12% Novex Tris–glycine gel (Invitrogen, Carlsbad, CA) and run for 60 min at 200 V. The proteins were then transferred onto a nitrocellulose membrane (Bio-Rad, Hercules, CA) for 1 h at 30 V. Protein transfer was confirmed by staining membranes with BLOT-FastStain (Chemicon, Temecula, CA). Subsequently, membranes were blocked in 5% Blotto non-fat dry milk in Tris buffer containing 1% Tween 20 for 1 h and probed overnight with anti-pEGFR, anti-pIGF1R, anti-pAkt, anti-Akt, anti-pGSK3b, anti-pNF-kB p65, anti-pJNK, anti-pP38, anti-pERK, anti-Bcl2, anti-Mcl-1 and anti-PARP. All primary antibodies were used at a dilution of 1:1000. After incubating the membranes with a secondary antibody (goat antirabbit IgG; 1:5000) for 1 h, chemiluminescent immunodetection was used. Signal was visualized by exposing membranes to HyBolt CL autoradiography film. All membranes were stripped and reprobed with anti-β-actin (1:1000) to check for differences in the amount of protein loaded in each lane. For each protein, at least three western assays were carried out. For quantitative determination of protein levels, densitometric measurements of western blot bands were performed using digitalized scientific software program UN-SCAN-IT (Silk Scientific, Orem, UT).

Analysis of DIM concentration in lung tissues

To determine if the concentrations of BRD that showed antiproliferative effects in cell culture studies could be achieved *in vivo* in the lung, groups of mice (three mice per group) received BRD by intranasal instillation at a dose of 2 mg per mouse and killed at the following time points: pretreatment, 1, 4, 8 and 24 h after treatment. Upon killing, lungs were harvested and kept immediately at −80°C until the day of analyses. For sample preparation, mouse lungs were thawed, blotted dry, weighed and homogenized (1:1 w/v) in 50 mM *N*-2-hydroxyethylpiperazine-*N*′-2-ethanesulfonic acid buffer at pH 7.4. Total homogenate for each mouse lung tissue was 600 μl. Aliquots (300 μl) of the tissue homogenates were transferred into clean 4 ml tubes and worked as described elsewhere in the literature (16). High-performance liquid chromatography–mass spectrometry was performed as described by Reed *et al.* (20). Selected ion monitoring for DIM was done at m/z 247–130. We followed the method described by Anderton *et al.* (21) to prepare the calibration curves and to determine the concentrations of DIM in lung tissues.

Tumor bioassay

Female A/J mice, 5–6 weeks of age, were obtained from The Jackson Laboratory (Bar Harbor, ME). Female mice are more docile and easier to work with than their male counterparts. Upon arrival (week 0), the mice were housed in the specific pathogen-free animal quarters of Research Animal Resources, University of Minnesota Academic Health Center, randomized into different groups and maintained on AIN-93G-pelleted diet. One week after arrival, the mice were switched to AIN-93G-powdered diet and treated with NNK (50 mg/kg, intraperitoneal, two doses, once a week in 0.1 ml physiological saline solution, groups 1 and 2) or the vehicle (0.1 ml of physiological saline solution, group 3). Beginning 1 week after the second dose of NNK, mice in group 2 have received intranasal instillations of BRD (2 mg per mouse), twice a week, in 50 μl physiological saline solution, 25 μl in each nostril. Intranasal instillation of BRD was carried out by placing droplets of the agent, using a 100 μl pipette, on the nasal tip of deeply anesthetized mice (using isoflurane). The deep abdominal breathing caused by isoflurane facilitated the intake of BRD droplets into the lower respiratory tract. Mice in group 3 received the vehicle for BRD in a similar manner. At week 10 of the study, the diet was changed from AIN-93G to AIN-93M. Diet consumption was measured twice weekly, and body weights were determined weekly. The study was terminated at week 27 by euthanizing the mice with an overdose of carbon dioxide. The lungs were harvested and tumors on the surface of the lung counted and their sizes determined under a dissecting microscope. Tumors on the surface of the right lobes of the lungs were microdissected, kept at −80°C and used, together with normal lungs from vehicle-treated mice, for western immunoblotting studies. The left lobes of the lungs were preserved in 10% buffered formalin and used for histopathological analyses.

Histology and Ki-67 immunohistochemistry

To determine the relative tumor area as a percentage of total lung area, sections of lung tissues were stained with hematoxylin and eosin and the percentage of lung tissue occupied by the tumors was determined in three different cross-sections of the lungs of three mice per group using the Image Pro program.

To assess the rate of cell proliferation in lung tissues by Ki-67 staining, 4 μm formalin-fixed paraffin sections were deparaffinized and antigen retrieved by incubating the slides in a pressure cooker in citrate buffer (pH 6.0) for 30 s at 121°C and 10 s at 90°C followed by cooling for 15 min. Endogenous peroxidase was blocked with 3% hydrogen peroxide for 15 min at room temperature. The sections were incubated with a universal protein block (DAKO) for 10 min, followed by a 60 min room temperature incubation with rat monoclonal antibody against mouse Ki-67 (DAKO) diluted at 1:50. Sections were then incubated for 30 min at room temperature with biotinylated antirat secondary antibody (Vector) diluted at 1:300. Binding was detected by incubating sections with streptavidin/horseradish peroxidase (DAKO) for 20 min at room temperature followed by diaminobenzidine chromogen application for 5 min at room temperature. Sections were counterstained with Mayer's hematoxylin (DAKO). For negative control slides, the primary antibody was substituted by Super Sensitive Negative Control Rat serum (Biogenix). The percentage of cells with Ki-67–positive nuclear staining (dense brown precipitate restricted to the nuclei) was determined with a Nikon Eclipse E800 microscope. Images were captured with an attached camera linked to a computer. Ten randomly selected fields were counted and each field corresponded to a total number of cells ranging from 700 to 1000.

Statistical analyses

Wilcoxon rank sum test was used for pairwise comparisons of the number of tumors on the surface of the lung (the group treated with NNK and received BRD versus the group treated with NNK only). Two-sided *P*-values ≤ 0.05 were considered statistically significant. For the analyses of tumor sizes and volumes, frequency of Ki-67-positive cells, the rate of cell proliferation, western immunoblotting results and apoptosis rate and the two-sided Student's *t*-test was used. Data are reported as mean ± SD of triplicate determinations. $*P < 0.05$ and $**P < 0.05$, compared with controls. All analyses were conducted in SAS 9.1.3.

Results

Effects of BRD on the growth of immortalized, premalignant and malignant human bronchial cells

To assess the antiproliferative activities of crystalline BRD, we used an *in vitro* model of lung tumorigenesis consisting of parental immortalized bronchial cell line (BEAS-2B) and its premalignant (1799 and 1198) and malignant (1170) derivatives. As depicted in Figure 1A, BRD significantly inhibited the growth of premalignant

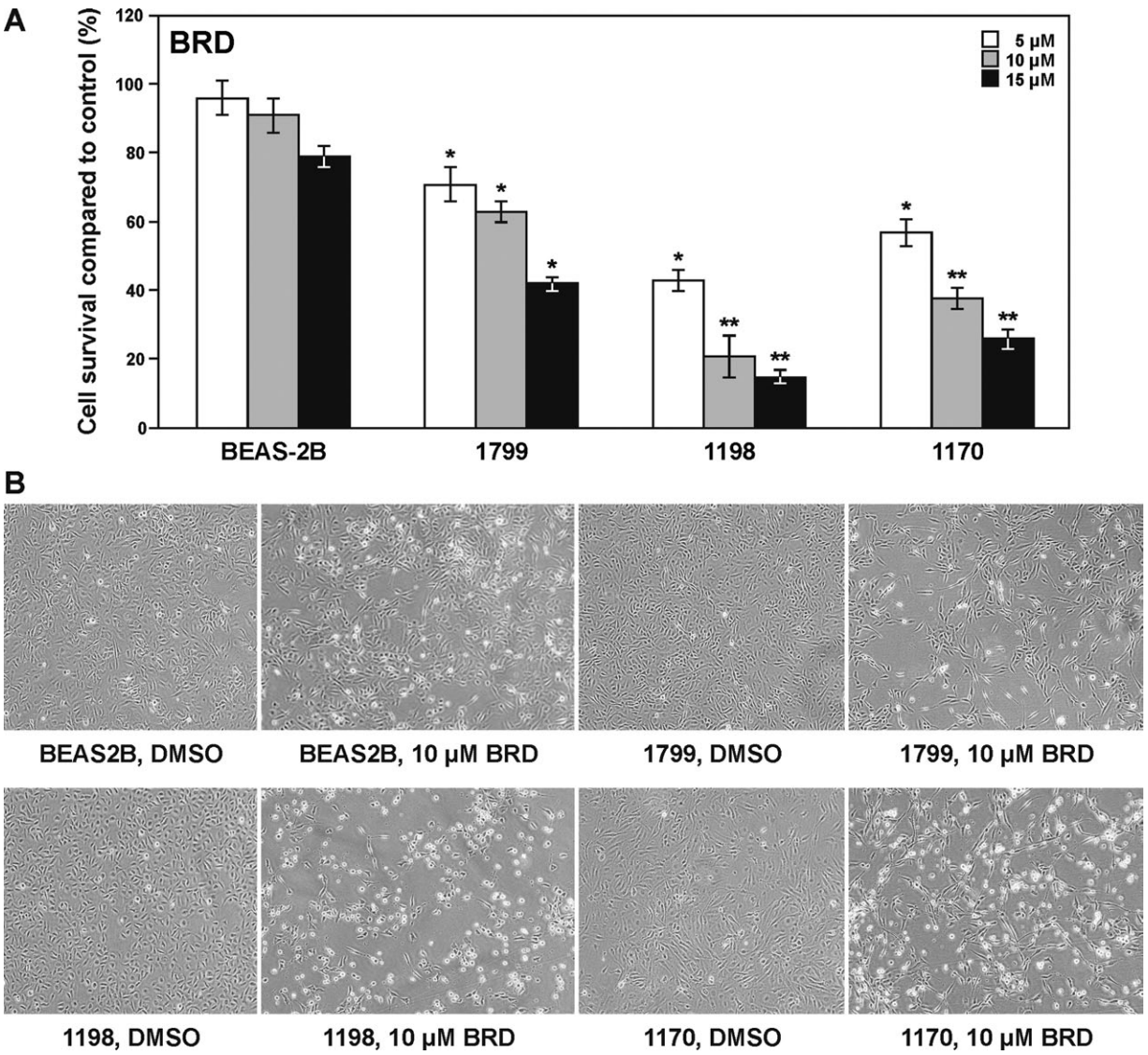

Fig. 1. Effect of BRD on the proliferation of parental immortalized human bronchial BEAS-2B cell line and its premalignant (1799 and 1198) and malignant (1170) derivatives. (**A**) BRD differentially inhibited the proliferation of 1799, 1198 and 1170 cells in a dose-dependent manner but only minimally affected the growth of BEAS-2B cells. Cells were grown on 96-well plates for 24 h and exposed to BRD (5, 10 or 15 μM) for 72 h and cell proliferation was determined by methylthiazoletetrazolium assay. The results were presented as mean ± SD of the percentage of the control. *$P < 0.05$ and **$P < 0.001$. (**B**) Images of BEAS-2B, 1799, 1198 and 1170 bronchial cells treated with DMSO or BRD (10 μM) for 72 h.

and malignant bronchial cells in a dose-dependent manner, but the effects in parental immortalized BEAS-2B cells were minimal. Among the three derivatives of BEAS-2B cells, 1198 cells were the most sensitive to the antiproliferative effects of BRD, followed by 1170, whereas 1179 cells were the least sensitive. Photomicrographs depicting BEAS-2B, 1799, 1198 and 1170 cells treated with DMSO or BRD are shown in Figure 1B.

Effects of BRD on cell proliferation- and apoptosis-related proteins

Because the PI3K/Akt pathway is an important regulator of cell proliferation and survival and a growing body of evidence implicates Akt activation in the early development of lung cancer (22–24), we sought to examine the effect of BRD on the Akt signaling pathway in parental BEAS-2B cells and premalignant 1198 cells. As depicted in Figure 2A, BRD differentially reduced levels of phosphorylated Akt as well as its downstream target phosphorylated GSK-3β in 1998 cells but not in parental BEAS-2B cells. BRD failed to modulate phosphorylation of epidermal growth factor receptor (EGFR) or Insulin-like growth factor 1 receptor (IGFR), which are upstream regulators of Akt, in both cell lines. Among members of mitogen-activated protein kinases, activation of c-jun N-terminal kinase (JNK) was increased, in particular in 1998 cells, but not that of p38 or extracellular signal-regulated kinase (Figure 2B). As markers for BRD induced apoptosis, we examined modulation of Bcl-2 and Mcl-1 and expression and poly (ADP ribose) polymerase (PARP) cleavage. In line with the cell proliferation assay, in 1198 cells but not in BEAS-2B cells, BRD markedly decreased level of Mcl-1 and induced the formation of the 89 kD, a signature PARP-1 fragment, a marker for apoptosis (Figure 3C). Levels of Bcl-2 were not affected by BRD.

Decreased Akt phosphorylation plays an important functional role in DIM-induced antiproliferative and apoptotic effects in transformed bronchial cells

To confirm if BRD-induced attenuation of Akt phosphorylation is indeed related to its antiproliferative and apoptotic activities in bronchial cells, 1198 cells were transfected with the vector alone or myr-Akt and subsequently treated with BRD. As shown in Figure 3A, compared with cells transfected with the vector, transfection of 1198 cells with myr-Akt led to an increase in pAkt and pGSK3β (lane 1), a dramatic attenuation of the effects of BRD on these proteins and

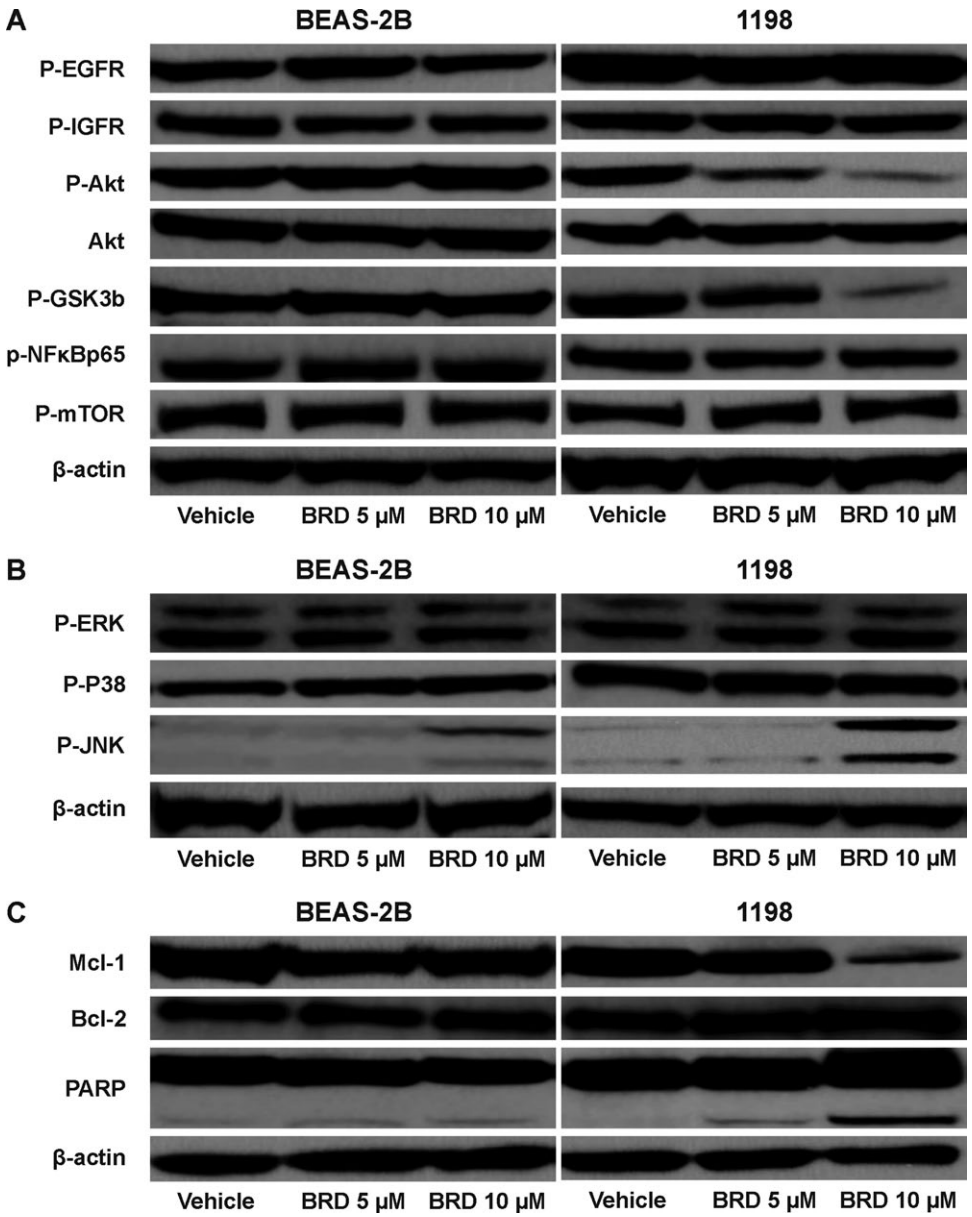

Fig. 2. Representative western immunoblots showing effects of BRD on proteins belonging to the PI3K/Akt signaling pathway (**A**), mitogen-activated protein kinase proteins extracellular signal-regulated kinase, p38 and JNK (**B**) and apoptosis pathway (**C**). Cells were treated with either DMSO or BRD (5 or 10 μM) for 72 h and cell lysates prepared thereof were analyzed by western immunoblotting as described in the Materials and methods section. At least three independent assays were carried out using cell lysates prepared on different days.

subsequent reduction in PARP cleavage (lane 3). Also, comparison of BRD-induced apoptosis in vector- and myr-Akt-transfected 1198 cells showed a 4-fold decrease of apoptotic cells upon exogenous overexpression of Akt (data not shown). Next, we determined the comparative efficacy of BRD and LY294002 on inhibition of Akt phosphorylation and cell death and if LY294002 enhances BRD-induced Akt inactivation and cell death. For this, 1198 cells were pretreated with the vehicle (0.1% DMSO), or low concentrations of LY294002 (10 or 20 μM), and after 1 h, cells were treated with DMSO or BRD (10 or 20 μM) for 24 h. As depicted in Figure 3B and C, treatment of 1198 cells with 10 μM of BRD or LY294002, individually, for 24 h caused a moderate but significant decrease in Akt phosphorylation and apoptosis and the efficacy of the two agents was similar. However, co-treatment with 10 μM LY294002 + 10 μM BRD caused a 2-fold increase in Akt inactivation and apoptosis compared with the effect of the individual agents. The enhancement by LY294002 of BRD-induced Akt inactivation and apoptosis was more clear in cells treated with 20 μM of BRD + 10 or 20 μM LY294002. The results depicted in Figure 3B and C further indicate that there was a good correlation between BRD/LY294002-induced inhibition of Akt phosphorylation and induction of apoptosis.

JNK activation does not play a role in DIM-mediated antiproliferative and apoptotic effects in bronchial cells

To determine if there is a correlation between BRD-induced JNK activation and the antiproliferative and apoptotic effects of the agent, we treated 1198 cells with a specific JNK inhibitor SP600125 and compared JNK activation status and apoptosis rate. As expected, treatment of cells with SP600125 reduced BRD-induced activation of JNK in a dose-dependent manner. However, the inhibitor, instead of suppressing apoptosis, significantly enhanced BRD-induced apoptosis. These results clearly indicated that JNK activation is not involved in the antiproliferative/apoptotic effects of BRD in bronchial cells.

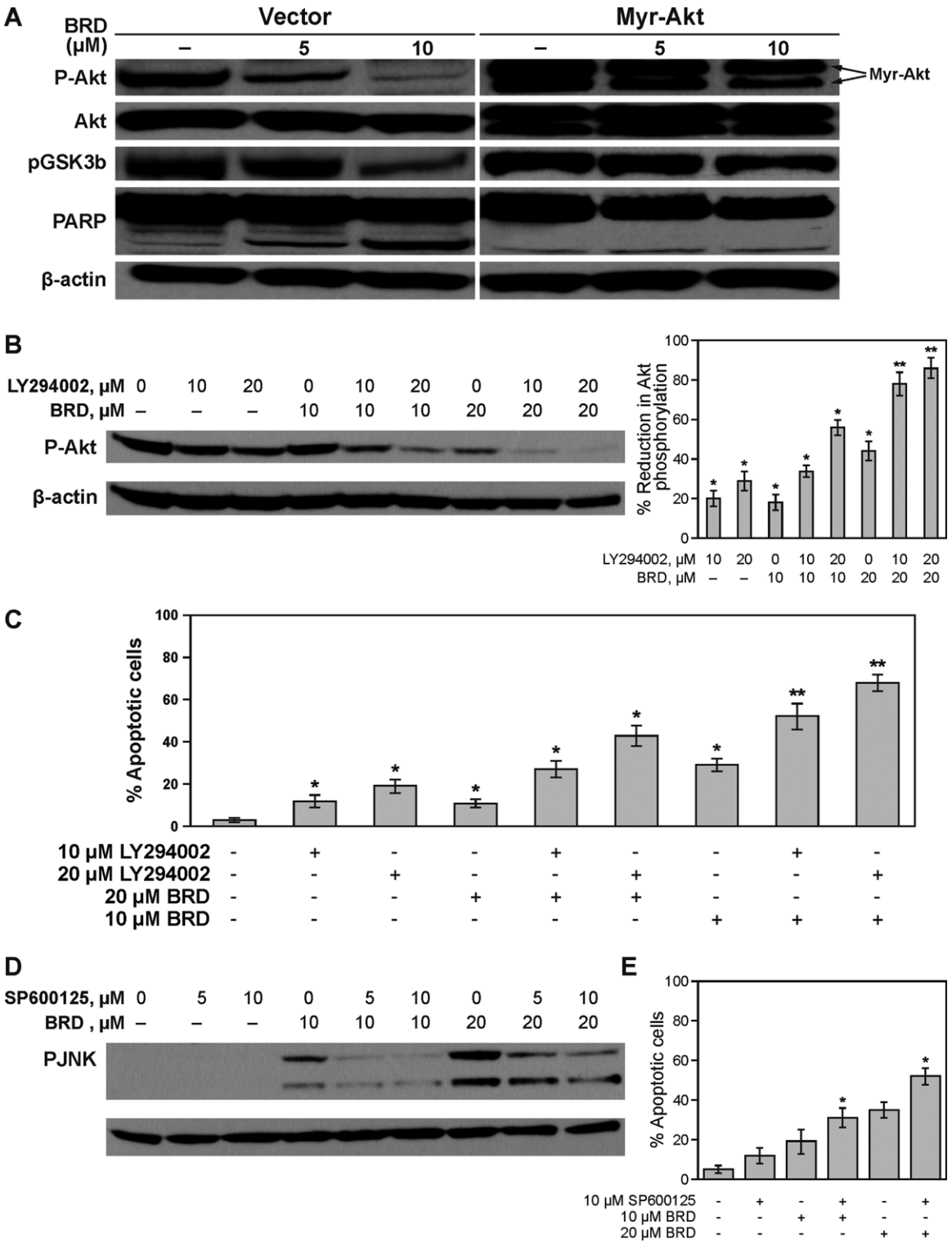

Fig. 3. Effects of genetic or pharmacological modulation of Akt expression or pharmacological modulation of JNK expression on BRD-induced Akt and JNK activation, respectively, and cell death. (**A**) Vector- or myr-Akt-transfected 1198 cells were treated with BRD and modulations of pAkt, Akt and pGSK3β expression and PARP cleavage were determined by western immunoblotting. (**B**) 1198 cells were pretreated with DMSO or LY29400220 and further exposed to DMSO or BRD for 24 h and modulation of Akt activation was assessed by western immunoblotting. To determine the relative activation of Akt in the different treatment groups, densitometric measurements of the bands were performed using digitalized scientific software program UN-SCAN-IT. $*P < 0.05$ and $**P < 0.001$, compared with DMSO-treated cells. (**C**) Rate of apoptosis in 1198 cells treated with LY29400220 and BRD, alone or individually, was analyzed by flow cytometry after staining with annexin V and PI. $*P < 0.05$ and $**P < 0.001$, compared with DMSO-treated cells. (**D**) Effect of the JNK inhibitor SP600125 on BRD-induced JNK activation. (**E**) Rate of apoptosis in 1198 cells pretreated with SP600125 and subsequently exposed to BRD for 24 h. Apoptosis rate was determined by flow cytometry after staining the cells with annexin V and PI. $*P < 0.05$ and $**P < 0.001$, compared with DMSO-treated cells.

Table I. Effects of intranasally administered BRD on NNK-induced lung tumors in A/J mice

Group	Treatment	No. of mice	Body weight (g)	Lung tumors			
				Incidence	Multiplicity	Reduction in multiplicity (%)[a]	*P**
1	NNK	20	22.2 ± 1.4	100	16.3 ± 2.9		
2	NNK + BRD	19	21.7 ± 1.8	100	4.6 ± 2.2	72	$P < 0.05$
3	Vehicle control	10	21.5 ± 1.2	30	0.3 ± 0.1		

All mice, with the exception of mice in group 3, received NNK (intraperitoneally, at a dose of 50 mg/kg, twice a week, for a total of two doses) in 0.1 ml physiological saline solution. Beginning 1 week after the last dose of NNK, mice in group 2 received BRD intranasally at a dose of 2 mg per mouse (0.6 mg pure DIM per mouse), twice a week, until termination of the study at week 27 (for a period of 24 weeks). Upon termination of the study, tumors on the surface of the lung were counted and tumor multiplicities were determined.
*Compared to group 1.
[a]Compared with group 1.

Accumulation of DIM in the lung

The marked antiproliferative and apoptotic effects of BRD in premalignant and malignant bronchial cells provided the impetus for further assessment of the potential chemopreventive activities of the agent in mice after direct delivery of the agent into the lung via intranasal instillation. Before carrying out tumor bioassay, we sought to determine if intranasal delivery of DIM would lead to accumulation of the agent in the lung at levels equivalent to those found to induce significant antiproliferative and apoptotic effects in bronchial cells. Pulmonary delivery of BRD, via intranasal instillation, at a dose level of 2 mg per mouse resulted in a maximal lung tissue DIM concentration of 23 μg/g lung tissue 1 h after treatment. Thereafter, the level of DIM in lung tissues decreased to 21, 18 and 12 μg/g at 4, 8 and 24 h post-administration, respectively. The amount of DIM accumulated in the lung corresponded to about 0.5–1% of the administered dose of DIM (assuming that a mouse lung weighs 200 mg and 0.6 mg of DIM per mouse was administered because the amount of DIM contained in BRD is 30%). Overall, these results showed rapid and prolonged accumulation of DIM in lung tissues after intranasal delivery of BRD and indicates the great potential of this route of drug administration for lung cancer chemoprevention.

Effect of BRD on body weight gain and NNK-induced lung tumor multiplicity, size and volume

Mice were treated intranasally with BRD for a total of 24 weeks according to the experimental design depicted in Figure 4A. Weekly body weight measurements throughout the study showed that BRD decreased body weight gain by a maximum of 2%, as compared with the control group, indicating that the administered dose of BRD was well tolerated (data not shown). In order to determine if long-term administration of BRD or isoflurane causes tissue damage, the upper and middle respiratory tract was examined macroscopically and microscopically by a certified pathologist, but no tissue alteration was noted.

Mice treated with NNK and given the vehicle had an average of 16.3 ± 2.9 lung tumors per mouse, whereas the group treated with NNK and given BRD intranasally developed 4.6 ± 2.2 lung tumors per mouse, corresponding to a significant reduction of tumor multiplicity by 72% (Table I). Likewise, classification of the tumors on the surface of the lung according to their sizes indicated that lung tumors with a size of >1 mm were almost completely abolished by BRD, whereas multiplicities of tumors with a size of 0.5–1 mm were reduced by 74% (Figure 4B). Photomicrographs of lung tissue sections showing the sizes and frequencies of lung tumors from mice treated with NNK alone or NNK plus BRD are shown in Figure 4C. Also, the area of lung tissue occupied by lung tumors was markedly reduced from 33% in the NNK group to 6% in the NNK plus BRD group, corresponding to a significant reduction by 82% (Figure 4D).

BRD inhibits the proliferation of lung tumor cells

One promising approach to determine the proliferation of tumor cells *in vivo* is immunohistochemical assessment of the nuclear antigen Ki-67, which is expressed in all phases of the cell cycle, except in resting cells. Representative micrographs of Ki-67-stained lung tissue sections from mice treated with physiological saline, NNK or NNK plus BRD and the percentage of cells with Ki-67–positive nuclear staining (dense brown precipitate restricted to the nuclei) are depicted in Figure 4E and F, respectively. The frequency of Ki-67–positive nuclei was significantly higher in NNK-induced lung tumors as compared with the level in normal lungs from vehicle-treated mice (12.3 ± 3.2% versus 0.3 ± 0.03%). Administration of BRD to NNK-pretreated mice reduced the frequency of Ki-67-positive cells to 3.1 ± 1.8% ($P < 0.001$). The antiproliferative effects of BRD were further confirmed through immunoblot analyses of Akt and GSK-3β activity and PARP cleavage in lung tumor tissues. As expected, NNK treatment led to activation of Akt and GSK-3β, but treatment with BRD significantly attenuated NNK-induced Akt and GSK-3β activation and caused PARP cleavage (Figure 4G and H).

Discussion

Although oral delivery is the most preferred route for the administration of chemopreventive agents, the oral bioavailability of most chemopreventive agents, including DIM, is low. In humans, administration of a single oral dose of 400–1200 mg indole-3-carbinol, the parent compound for DIM, resulted in a peak plasma DIM concentration of 0.25–2.5 μmol/l (20), which is much lower than the concentrations of DIM (40–100 μmol/l) found to induce antiproliferative and apoptotic effects in cell line models (3). Similarly, administration of BRD to healthy subjects at a maximally tolerated dose level (200 mg per person) led to plasma DIM concentration of only 0.5 μmol/l (14); increasing the dose of BRD to 300 mg per person failed to increase the plasma concentration of the agent. According to these reports, oral administration of DIM might not result in therapeutically relevant concentrations of the agent in the lung tissues. This situation prompted the search for a more effective route for the delivery of DIM to the lung. One very promising route of drug administration to deliver BRD to the lung is intranasal instillation in view of the possibility to administer the agent directly to the lung and thereby enhancing its bioavailability to the lung, large surface area and rich vascular network of the lung, the ease of administration, a rapid onset of action and the avoidance of potential gastrointestinal and hepatic first-pass effects (25). In earlier works, pulmonary delivery of chemopreventive agents in a form of aerosol showed a remarkable efficacy in suppressing lung tumorigenesis (26–28). However, aerosol administration of chemopreventive agents is expensive and technically demanding.

This work has clearly demonstrated that intranasal delivery is a useful approach to improve the bioavailability of DIM in lung tissues and to overcome the side effects related to high doses of the agent. Intranasal instillation of 2 mg BRD per mouse (0.6 mg pure DIM per mouse), which is less than the maximum tolerated dose of DIM in humans (14), when extrapolated to a human equivalent dose using body surface area normalization method (29), resulted in a mean lung tissue concentration of 19 μg/g (77 μmol/l). This concentration of DIM is similar to the level of DIM reported in lung tissues of mice

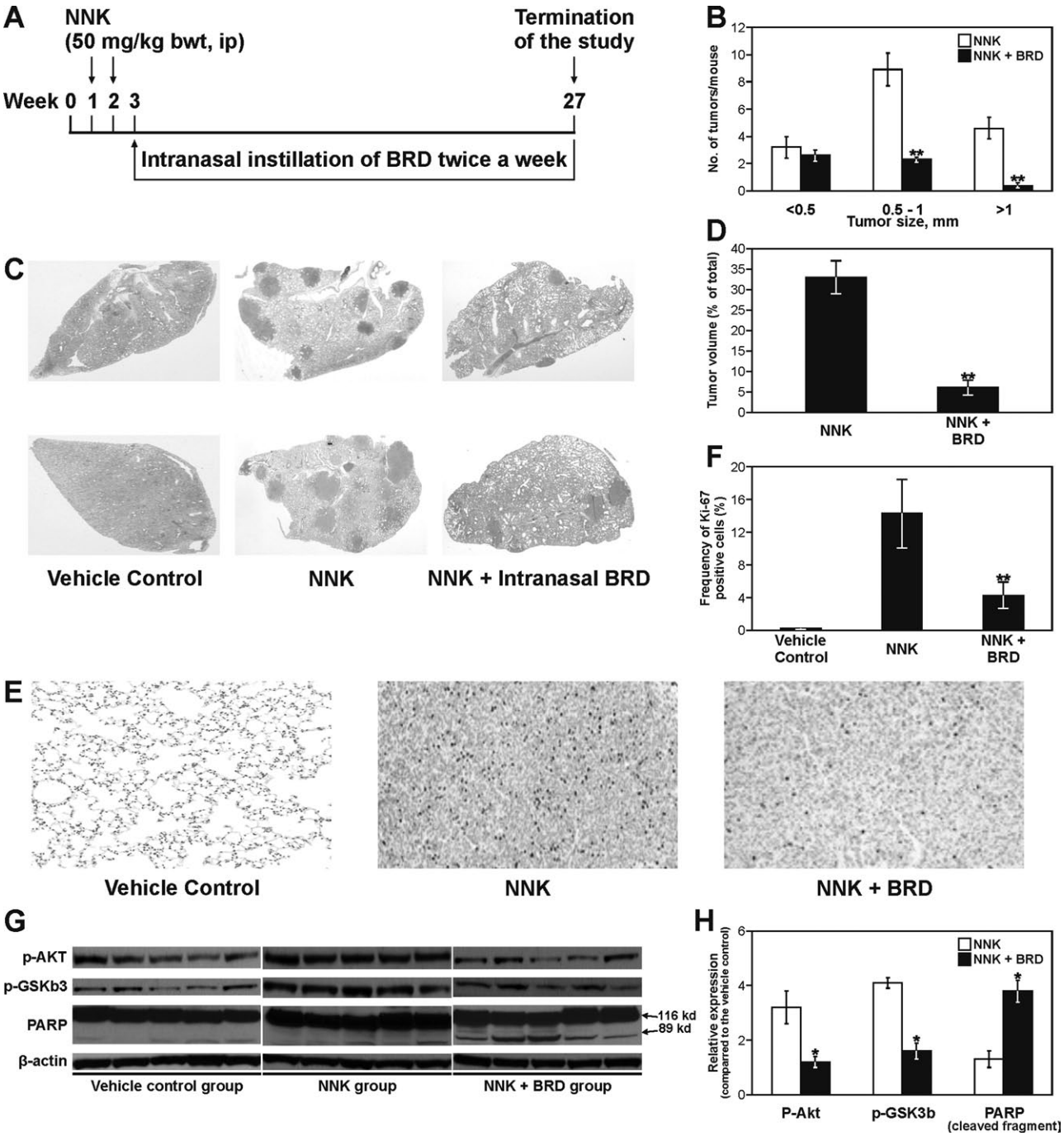

Fig. 4. Effects of BRD on NNK-induced lung tumors in A/J mice. (**A**) Experimental design of lung tumor bioassay. (**B**) Effects of BRD on the growth of lung tumors. The size of surface tumors on lungs of mice was estimated using the calibrated scale in the eyepiece of a dissecting microscope. Each tumor was assigned to one of the following categories: <0.5, 0.5–1 and >1 mm; $^{**}P < 0.001$. (**C**) Images of representative cross-sections of lung tissues from control mice and mice treated with NNK alone, or NNK plus BRD (2 mg per mouse). Lung tumors from NNK plus BRD-treated mice were fewer and smaller than tumors from mice treated with NNK alone. (**D**) Effects of BRD on the volume of NNK-induced lung tumors. Sections of lung tissues were stained with hematoxylin and eosin and the percentage of lung tissue occupied by the tumors was determined in three different cross-sections of the lungs of three mice per group using the Image Pro program; $^{**}P < 0.001$. (**E**) Photomicrographs (×20) of Ki-67-stained lung tissues from mice treated with vehicle control, NNK or NNK plus BRD. Lung tissues were cut into 4-μm sections and stained with Ki-67 antibody and counterstained with hematoxylin. Images were captured with a camera attached to a Nikon Eclipse E800 microscope. (**F**) Quantitative assessment of Ki-67–positive cells, representing the percentage of cells that stained positive for Ki-67. The Ki-67 labeling index was calculated as described in Materials and methods. Columns: mean; bars: SD; $^{**}P < 0.001$. (**G**) Western immunoblots of lung tissues. Lung tissue lysates prepared from whole normal lung tissues (vehicle control) or microdissected tumors from mice treated with NNK or NNK + BRD, five mice each, were loaded onto 4–12% sodium dodecyl sulfate–polyacrylamide gel electrophoresis and processed as described in Materials and methods. Equal loading of protein was confirmed by stripping the immunoblot and reprobing it for β-actin. (**H**) Quantitative data showing levels of pAkt, pGSK3b and cleaved PARP in NNK- and NNK + BRD-treated mice relative to the level in vehicle-treated mice. Protein band density was determined with a scanning densitometer (Personal Densitometer; Molecular Dynamics, Sunnyvale, CA). Data were generated from three independent experiments. $^{*}P < 0.05$, compared with the NNK group.

given BRD by oral gavage at a 10-fold higher dose (16), thus clearly showing the higher bioavailability of intranasally administered BRD. The amount of DIM achieved in the lung tissues is also equivalent to the concentration of DIM used in most cell line models (3). The effect of BRD on lung tumor multiplicity observed in this study was comparable with that we reported earlier (13) in mice given BRD in the diet at a 9-fold higher dose level (30 μmol/g diet, approximately, 5.4 mg per mouse) than the amount delivered via the intranasal route. In the same dietary supplementation study, BRD was also added to the diet at a dose level equivalent to what was administered intranasally, but the tumor multiplicity was reduced only by 5%. These results clearly indicate that the higher bioavailablility of DIM, as a result of direct delivery of BRD into the lung, was translated into greater chemopreventive efficacy. Our results are in line with a previous report in which intranasal instillation of the chemopreventive agent deguelin to mice led to a more rapid increase and higher concentration of the agent in lung tissues as compared with mice given the agent by oral gavage (30).

To determine the mechanisms of antiproliferative and apoptotic activities of BRD in transformed bronchial cells, we assessed the effect of the agent on Akt and related proteins. The PI3K/Akt signaling pathway is a central pathway that integrates and modulates several signaling pathways related to cell growth and survival including receptor tyrosine kinase signaling, NF-kB signaling and extracellular signal-regulated kinase signaling cascade (31,32). The binding of growth factors to their receptor tyrosine kinase or G protein-coupled receptors stimulates the phosphorylation of PI3K, which then converts phosphatidylinositole-4,5 bisphosphonate [PI(4,5)P2] to PI(3,4,5)P3. Interaction of Akt with PI (3–5)P3 via its PH domain, results in its full activation through phosphorylation at two key sites, threonine 308 and serine 473 (31,32). Once activated, it dissociates from the plasma membrane and translocates into the cytosol to regulate activities of various proteins involved in cell survival and proliferation. Although EGFR and IGFR are principal upstream regulators of Akt (33,34), in this study, BRD did not modulate EGFR or IGFR activation, suggesting that another signaling molecule downstream of EGFR and IGFR, probably PI3K, is the potential target of BRD. Indeed, we have shown that PI3K inhibition by LY294002, a highly selective PI3K inhibitor that is structurally unrelated to BRD, inhibited the growth and survival of malignant bronchial cells. These results indicate that PI3K inhibition alone is sufficient for the chemopreventive activities of BRD in transformed bronchial cells and suggest that downregulation of PI3K may be a mechanism for BRD-mediated inhibition of Akt activation, cell proliferation and survival. Another evidence for the link between the chemopreventive activities of BRD and inhibition of the PI3K/Akt pathway is that exogenous overexpression of Akt attenuated BRD-induced suppression of Akt and GSK-3β activation, PARP cleavage and apoptotic effects. GSK-3 is a critical downstream target of the PI3K/Akt pathway and its phosphorylation by activated Akt leads to positive regulation of WNT signaling and protein synthesis (35). PARP cleavage is consistent with suppression of Akt activation and indicates the apoptotic effects of BRD.

Although an overwhelming evidence indicates the role of the JNK pathway in apoptosis induction and tumor suppression (36), JNKs, in particular JNK1, have been found to play a role in malignant transformation of cells and in tumorigenesis. For instance, JNK1 has been viewed as a pivotal kinase that promotes the development of tobacco smoke–induced lung tumors because the ablation of JNK1 alone reduced the effect of tobacco smoke on both the lung tumor multiplicity and the tumor size (37). In this study, although JNK was markedly activated upon treatment of transformed bronchial cells with BRD and this effect was suppressed by SP600125, the pharmacological inhibitor of JNK, BRD-induced apoptosis was not decreased by SP600125. Instead, BRD-induced apoptosis was enhanced by the JNK inhibitor. These results clearly indicate that increased JNK activation does not play a role in the antiproliferative and apoptotic activities of BRD in transformed bronchial cells. In previous reports, JNK has been shown to be activated and/or overexpressed in an antiapoptotic manner in various cancers, and JNK inhibition has increased anticancer effects of proteasome inhibitors in pancreatic cancer cells (38,39). However, the antiproliferative and apoptotic effects of BRD in the face of JNK activation observed in this study are unclear.

In summary, we showed in this study that intranasal delivery of BRD at a very low dose level had the same antitumor efficacy with an oral dose of the agent given at 10-fold higher dose level in our previous study (13) and these effects are mediated, at least in part, through inhibition of the PI3K/Akt signaling pathway. Moreover, because BRD is directly given to the lung at a reduced dose and frequency, potential toxic effects are reduced. Because inhalation therapy has been found to be a valuable tool in the targeted therapy of chronic pulmonary diseases such as asthma and chronic obstructive pulmonary disease, intranasal delivery of BRD and other chemopreventive agents could be a viable approach for clinical lung cancer chemoprevention trials in subjects at high risk for lung cancer.

Funding

National Cancer Institute/National Institutes of Health grant (5R01CA128801-04 to F.K.).

Acknowledgements

We wish to thank Dr Michael Zeligs for the generous gift of BRD. We are also grateful to the Comparative Pathology Core of Masonic Cancer Center, University of Minnesota, for the help in the histopathological analyses of lung tissues.

Conflict of Interest Statement: None declared.

References

1. Siegel,R. *et al.* (2012) Cancer statistics, 2012. *CA. Cancer J. Clin.*, **62**, 10–29.
2. Jemal,A. *et al.* (2010) Global patterns of cancer incidence and mortality rates and trends. *Cancer Epidemiol. Biomarkers Prev.*, **19**, 1893–1907.
3. Banerjee,S. *et al.* (2011) Attenuation of multi-targeted proliferation-linked signaling by 3,3'-diindolylmethane (DIM): from bench to clinic. *Mutat. Res.*, **728**, 47–66.
4. Banerjee,S. *et al.* (2009) 3,3'-Diindolylmethane enhances chemosensitivity of multiple chemotherapeutic agents in pancreatic cancer. *Cancer Res.*, **69**, 5592–5600.
5. Ali,S. *et al.* (2009) Sensitization of squamous cell carcinoma to cisplatin induced killing by natural agents. *Cancer Lett.*, **278**, 201–209.
6. Fan,S. *et al.* (2009) Low concentrations of diindolylmethane, a metabolite of indole-3-carbinol, protect against oxidative stress in a BRCA1-dependent manner. *Cancer Res.*, **69**, 6083–6091.
7. Kong,D. *et al.* (2008) Mammalian target of rapamycin repression by 3,3'-diindolylmethane inhibits invasion and angiogenesis in platelet-derived growth factor-D-overexpressing PC3 cells. *Cancer Res.*, **68**, 1927–1934.
8. Wang,Z. *et al.* (2008) Induction of growth arrest and apoptosis in human breast cancer cells by 3,3-diindolylmethane is associated with induction and nuclear localization of p27kip. *Mol. Cancer Ther.*, **7**, 341–349.
9. Rahman, K.W. *et al.* (2009) 3,3'-diindolylmethane enhances taxotere-induced apoptosis in hormone refractory prostate cancer cells through surviving down regulation. *Cancer Res.*, **69**, 4468–4475.
10. Rahman,K.M. *et al.* (2007) Inactivation of NF-kappaB by 3,3'-diindolylmethane contributes to increased apoptosis induced by chemotherapeutic agent in breast cancer cells. *Mol. Cancer Ther.*, **6**, 2757–2765.
11. Cho,H.J. *et al.* (2011) 3,3'-Diindolylmethane inhibits prostate cancer development in the transgenic adenocarcinoma mouse prostate model. *Mol. Carcinog.*, **50**, 100–112.
12. Sepkovic,D.W. *et al.* (2009) Diindolylmethane inhibits cervical dysplasia, alters estrogen metabolism, and enhances immune response in the K14-HPV16 transgenic mouse model. *Cancer Epidemiol. Biomarkers Prev.*, **18**, 2957–2964.
13. Kassie,F. *et al.* (2007) Indole-3-carbinol inhibits 4-(methylnitrosamino)-1-(3-pyridyl)-1-butanone plus benzo(a)pyrene-induced lung tumorigenesis in A/J mice and modulates carcinogen-induced alterations in protein levels. *Cancer Res.*, **67**, 6502–6511.
14. Reed,G.A. *et al.* (2008) Single-dose pharmacokinetics and tolerability of absorption-enhanced 3,3'-diindolylmethane in healthy subjects. *Cancer Epidemiol. Biomarkers Prev.*, **17**, 2619–2624.

15. Zeligs, M.A. *et al.* (2000) Compositions and methods of adjusting steroid hormone metabolism through phytochemicals. U.S. patent 6,086,915.
16. Anderton,M.J. *et al.* (2004) Physiological modeling of formulated and crystalline 3,3'-diindolylmethane pharmacokinetics following oral administration in mice. *Drug Metab. Dispos.*, **32**, 632–638.
17. Hecht,S.S. *et al.* (1983) Effects of alpha-deuterium substitution on the mutagenicity of 4-(methyl-nitrosamino)-1-(3-pyridyl)-1-butanone (NNK). *Carcinogenesis*, **4**, 305–310.
18. Reeves,P.G. *et al.* (1993) AIN-93 purified diets for laboratory rodents: final report of the American Institute of Nutrition ad hoc writing committee on the reformulation of the AIN-76A rodent diet. *J. Nutr.*, **123**, 1939–1951.
19. Klein-Szanto,A.J. *et al.* (1992) A tobacco-specific N-nitrosamine or cigarette smoke condensate causes neoplastic transformation of xenotransplanted human bronchial epithelial cells. *Proc. Natl. Acad. Sci. U.S.A.*, **89**, 6693–6697.
20. Reed,G.A. *et al.* (2006) Single-dose and multiple-dose administration of indole-3-carbinol to women: pharmacokinetics based on 3,3'-diindolylmethane. *Cancer Epidemiol. Biomarkers Prev.*, **15**, 2477–2481.
21. Anderton,M.J. *et al.* (2003) Liquid chromatographic assay for the simultaneous determination of indole-3-carbinol and its acid condensation products in plasma. *J. Chromatogr. B Analyt. Technol. Biomed. Life Sci.*, **787**, 281–291.
22. Tsao,A.S. *et al.* (2003) Increased phospho-AKT (Ser(473)) expression in bronchial dysplasia: implications for lung cancer prevention studies. *Cancer Epidemiol. Biomarkers Prev.*, **12**, 660–664.
23. Massion,P.P. *et al.* (2004) Early involvement of the phosphatidylinositol 3-kinase/Akt pathway in lung cancer progression. *Am. J. Respir. Crit. Care Med.*, **170**, 1088–1094.
24. Gustafson,A.M. *et al.* (2010) Airway PI3K pathway activation is an early and reversible event in lung cancer development. *Sci. Transl. Med.*, **2**, 26ra25.
25. Chien,Y.W. (1989) Nasal systemic drug delivery. In Chien,Y.W. (ed) *Drugs and the Pharmaceutical Sciences*. Marcel Dekker, New York, pp. 1–26.
26. Fu,H. *et al.* (2009) Lung cancer inhibitory effect of epigallocatechin-3-gallate is dependent on its presence in a complex mixture (polyphenon E). *Cancer Prev. Res. (Phila).*, **2**, 531–537.
27. Fu,H. *et al.* (2011) Chemoprevention of lung carcinogenesis by the combination of aerosolized budesonide and oral pioglitazone in A/J mice. *Mol. Carcinog.*, **50**, 913–921.
28. Ichite,N. *et al.* (2010) Inhalation delivery of a novel diindolylmethane derivative for the treatment of lung cancer. *Mol. Cancer Ther.*, **9**, 3003–3014.
29. Reagan-Shaw,S. *et al.* (2008) Dose translation from animal to human studies revisited. *FASEB J.*, **22**, 659–661.
30. Woo,J.K. *et al.* (2009) Liposomal encapsulation of deguelin: evidence for enhanced antitumor activity in tobacco carcinogen-induced and oncogenic K-ras-induced lung tumorigenesis. *Cancer Prev. Res. (Phila).*, **2**, 361–369.
31. Bartholomeusz,C. *et al.* (2012) Targeting the PI3K signaling pathway in cancer therapy. *Expert Opin. Ther. Targets*, **16**, 121–130.
32. Papadimitrakopoulou,V. (2012) Development of PI3K/AKT/mTOR pathway inhibitors and their application in personalized therapy for non-small-cell lung cancer. *J. Thorac. Oncol.*, **7**, 1315–1326.
33. Yeh,J. *et al.* (2008) Selective inhibition of SCLC growth by the A12 anti-IGF-1R monoclonal antibody correlates with inhibition of Akt. *Lung Cancer*, **60**, 166–174.
34. Arteaga,C.L. (2002) Epidermal growth factor receptor dependence in human tumors: more than just expression? *Oncologist*, **7** (suppl. 4), 31–39.
35. Ougolkov,A.V. *et al.* (2006) Targeting GSK-3: a promising approach for cancer therapy? *Future Oncol.*, **2**, 91–100.
36. Liu,J. *et al.* (2005) Role of JNK activation in apoptosis: a double-edged sword. *Cell Res.*, **15**, 36–42.
37. Takahashi,H. *et al.* (2010) Tobacco smoke promotes lung tumorigenesis by triggering IKKbeta- and JNK1-dependent inflammation. *Cancer Cell*, **17**, 89–97.
38. Li,M. *et al.* (2007) Thymosinalpha1 stimulates cell proliferation by activating ERK1/2, JNK, and increasing cytokine secretion in human pancreatic cancer cells. *Cancer Lett.*, **248**, 58–67.
39. Sloss,C.M. *et al.* (2008) Proteasome inhibition activates epidermal growth factor receptor (EGFR) and EGFR-independent mitogenic kinase signaling pathways in pancreatic cancer cells. *Clin. Cancer Res.*, **14**, 5116–5123.

Received October 13, 2012; revised November 15, 2012; accepted December 4, 2012